

# **Theoretical evaluation of some compounds with antifungal effect as corrosion inhibitors for copper in nitric acid solution: DFT calculations**

---

## **ABSTRACT**

Quantum chemical calculations based on density functional theory (DFT) at the B3LYP/6-31G (d,p) basis set were used to study the inhibition performance of four antifungal organic molecules in copper corrosion in 1M nitric acid solution. The quantum chemical descriptors analysis shows that the investigated compounds have good inhibitory abilities in combating copper corrosion. It results that the inhibition efficiency of these molecules is a function of highest occupied molecular orbital (HOMO), lowest unoccupied molecular orbital (LUMO) and the energy gap. The inhibition performance of these molecules increases when the energy gap decreases. Finally, the areas containing N, S and C atoms are the most likely sites to bind to the copper surface either by donating or receiving electrons.

*Keywords: Quantum chemical calculations, density functional theory, inhibition performance, antifungal, copper corrosion*

## **1. INTRODUCTION**

In the last few decades, many experimental investigations have been undertaken with the common goal of revealing inhibitive action of a series of chemical compounds [1]. Although experimental studies are straightforward, they are often tedious, time-consuming and expensive. Theoretical investigations based on quantum chemical calculations have been proposed as a way for predicting a number of molecular parameters directly related to the corrosion inhibiting property of any chemical compound [2–5]. Many reviews have been recently reported considering the use of quantum chemical methods and computational techniques to explain the corrosion inhibitors behavior [6-10]. Some researches in this field have proved that the protective activity of an inhibitor generally relies on several physicochemical and electronic properties of the protective molecules, in particular, its organic functional groups, steric properties, electron density of the contributing atoms and the orbital characteristic of electron sharing [11-13].

Indeed a number of these inhibitors are also highly hazardous to health and the environment, and are the subject of increasing ecological scrutiny and strict environmental regulations. Current research efforts are now focusing on the development of non-toxic, low-cost and environmentally friendly corrosion inhibitors as alternatives. The required electronic structural features of corrosion inhibitors, such as the presence of heteroatoms, extensive

conjugation, and substituted heterocycles, are readily found in biochemical compounds used as drugs [14,15]. Interestingly, some drugs have been shown to be effective in inhibiting certain metals.

In order to respect the recommendations on environment preservation and to promote the health of all, this work has been focused on studying the inhibitory power of four therapeutic molecules with antifungal (figure 1) effect in copper corrosion in an acidic environment. The choice of this metal is based on its massive use in several sectors and on its physicochemical properties.

Quantum chemistry calculations based essentially on Density Functional Theory (DFT) were used in this study to explain how these molecules will be able to protect copper in an acidic environment.

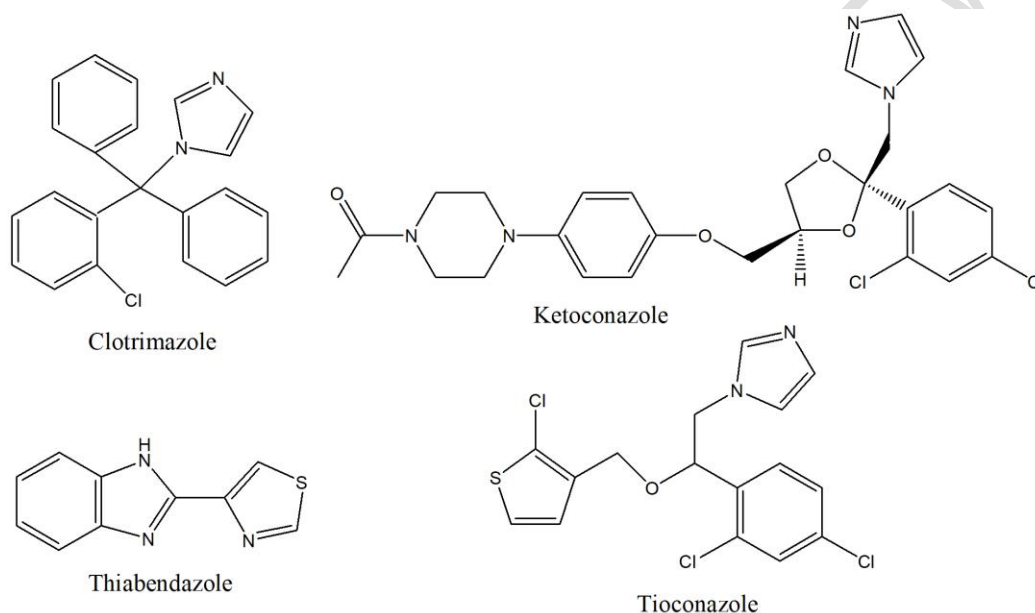


**Figure 1.** The molecular structures of the investigated inhibitors

## 2. METHODS

### Theoretical calculations details

In this work, theoretical calculations are based on Density Functional Theory (DFT). All calculations in the gas and aqueous phases were performed using the Gaussian 09 software suite [16]. The geometry optimizations were carried out using the hybrid functional B3LYP (Beckes three-parameter with Lee–Yang–Parr) with 6-31G (d) basis set [17, 18].

Moreover the quantum chemical parameters such as as highest occupied molecular orbital energy ( $E_{\text{HOMO}}$ ), lowest unoccupied molecular orbital energy ( $E_{\text{LUMO}}$ ), energy gap ( $\Delta E$ ), ionization potential (I), electron affinity (A) dipole moment ( $\mu$ ), electronegativity  $\chi$ , hardness  $\eta$ , softness  $S$ , electrophilicity index  $\omega$ , Fukui function  $f_k^+$  or  $f_k^-$  and dual descriptor ( $\Delta f_k^+$  or  $\Delta f_k^-$ ).

The energy gap is determined by the following expression:

$$\Delta E = E_{LUMO} - E_{HOMO} \quad (1)$$

The ionization potential (I) and electron affinity (A) of the inhibitors are calculated according to Koopman's theorem [19]

$$I = -E_{HOMO} \quad (2)$$

$$A = -E_{LUMO} \quad (3)$$

The electronegativity ( $\chi$ ) [20] and the hardness ( $\eta$ ) [21] of the inhibitors were estimated using the value of I and A that given by:

$$\chi = -\mu_p = \left( \frac{\partial E}{\partial N} \right)_{v(r)} \quad (4)$$

$$\chi = \frac{I+A}{2} \quad (5)$$

$$\eta = \frac{I-A}{2} \quad (6)$$

The global softness (S) is obtained from the equation [21]:

$$S = \frac{1}{\eta} = \frac{2}{I-A} \quad (7)$$

The global electrophilicity index ( $\omega$ ) [22] is defined as follows:

$$\omega = \frac{(I+A)^2}{4(I-A)} \quad (8)$$

The fraction of electrons transferred ( $\Delta N$ ) from the inhibitor molecule to the metal was performed according to Pearson's electronegativity relationship [23]:

$$\Delta N = \frac{\chi_{Cu} - \chi_{inh}}{2(\eta_{Cu} + \eta_{inh})} \quad (9)$$

where  $\chi_{Cu}$  and  $\eta_{Cu}$ ,  $\chi_{inh}$  and  $\eta_{inh}$  denote the electronegativity and hardness of copper and the inhibitor molecule respectively. In our case we use the theoretical value of  $\chi_{Cu} = 4.98$  eV/mol and  $\eta_{Cu} = 0$  [24] assuming that for a metallic charge  $I = A$  [25], for the calculation of the number of transferred electrons.

To locate the sites of reactivity within each molecule, the Fukui functions were determined from Mulliken charges. Fukui functions, which can be determined using the finite difference approximation:

$$\text{Nucleophilic attack} \quad f_k^+ = q_k(N+1) - q_k(N) \quad (13)$$

$$\text{Electrophilic attack} \quad f_k^- = q_k(N) - q_k(N-1) \quad (14)$$

where  $q_k(N+1)$ ,  $q_k(N)$  and  $q_k(N-1)$  are the electronic population of atom k in  $(N+1)$ ,  $N$  and  $(N-1)$  electrons systems.

The dual descriptor was introduced to unambiguously explain the sites of local reactivity [26,27]. this descriptor can be determined by the following relations:

$$\Delta f_k(r) = \left( \frac{\partial f_k(r)}{\partial N} \right)_{v(r)} \quad (15)$$

$$\Delta f_k(r) = f_k^+ - f_k^- \quad (16)$$

### 3. RESULTS AND DISCUSSION

#### 3.1 Molecules optimized forms

The optimized structures of the studied molecules performed by DFT with labels by B3LYP/6-31G (d) are represented by the figure 2.

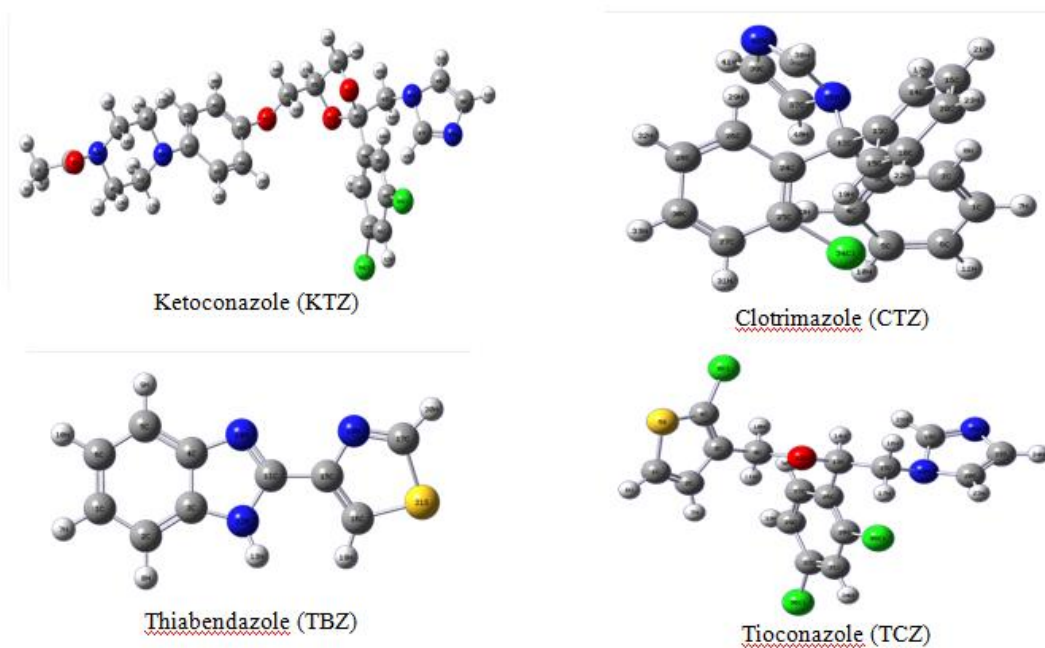


**Figure 2. Optimized structure of KTZ, CTZ, TBZ and TCZ calculated with B3LYP/6-31G (d)**

#### 3.2 Global reactivity parameters analysis

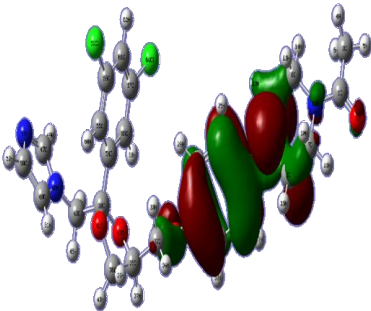
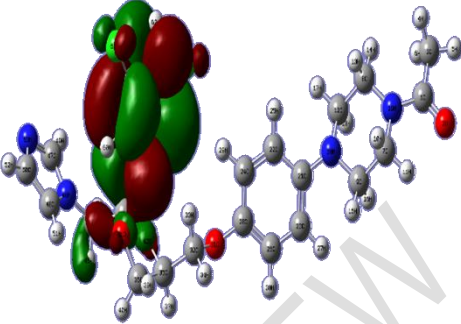
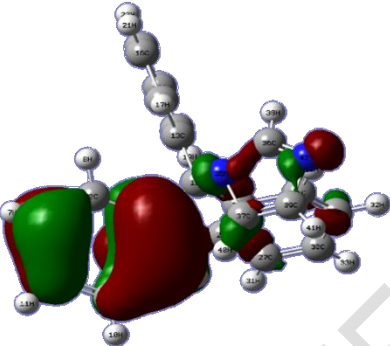
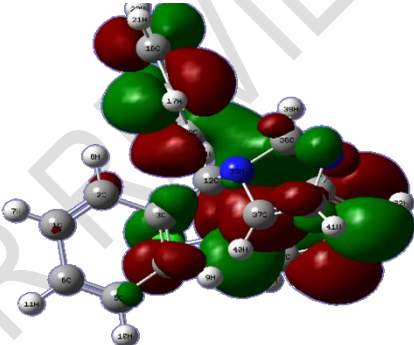
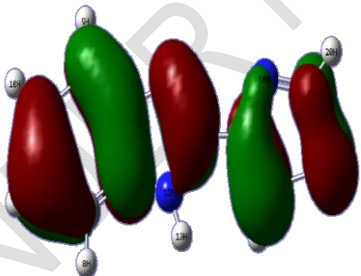
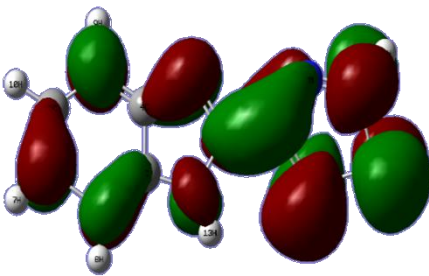
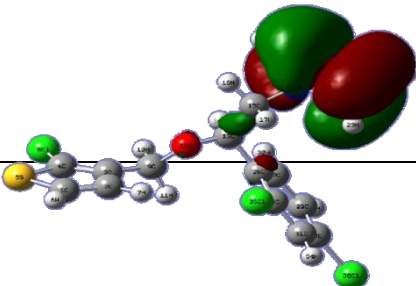
The values of the calculated quantum chemical global parameters with the B3LYP/6-31G (d) are listed in table 1.

**Table 1. Quantum chemical parameters of the studied compounds calculated using B3LYP/6-31G (d).**

Parameters	Ketoconazol	Clotrimazol	Thiabendazol	Tioconazol
$E_{HOMO}$ (eV)	-5,5553	-5,9233	-5,8341	-6,1246
$E_{LUMO}$ (eV)	-0,9365	-0,7115	-1,3410	-1,1788
Energy gap $\Delta E$ (eV)	4,6188	5,2118	4,4931	4,9458
Dipole moment $\mu$ (D)	6,0900	2,3297	3,4576	3,3014
Ionization energy I (eV)	5,5553	5,9233	5,8341	6,1246
Electron affinity A (eV)	0,9365	0,7115	1,3410	1,1788
Electronegativity $\chi$ (eV)	3,2459	3,3174	3,5875	3,6517
Hardness $\eta$ (eV)	2,3094	2,6059	2,2466	2,4728
Softness $S$ (eV) <sup>-1</sup>	0,4330	0,3837	0,4451	0,4043
Fraction of electron transferred $\Delta N$	0,3754	0,3190	0,3099	0,2685
Electrophilicity index $\omega$	2,2810	2,1113	2,8644	2,6962
Total energy $E_T$ (Ha)	-2447.7078	-1417.9664	-947.6897	-2580.8709

According the molecular orbitals theory, chemical reactivity is a function of the interaction between the HOMO and LUMO levels of the reacting species [28].  $E_{HOMO}$  is a quantum chemical parameter which indicates that a molecule can give to a suitable acceptor system of low energy molecular orbital empty [29]. The analysis of the values obtained show that Ketoconazol has the highest value of  $E_{HOMO}$ , however it could have the best ability to donate electrons to the metal.

These molecules do not only supply electrons to the «d» orbitals of metal ions such as  $Cu^{2+}([Ar] 3d^9)$ , but they can also receive electrons from these «d» orbitals, leading to a mutual exchange of electrons [30]. In our case, the low  $E_{LUMO}$  values show that these molecules tend to receive electrons. The lower the values of  $E_{LUMO}$ , the more probable it is that the molecules accepts electrons. The binding capacity of the inhibitor to the metal surface increases with increasing HOMO and decreasing LUMO energy values because the geometry of the inhibitor's base state and the nature of its frontier molecular orbitals, HOMO and LUMO, are involved in the inhibition process[30]. It should be noted that the electron density of the HOMO location in each molecule is mainly distributed near the nitrogen (N) and oxygen (O) atoms showing that these are the preferred sites for adsorption, whereas the LUMO density was distributed almost of the entire molecules. The HOMO-LUMO diagrams of the molecules are shown in **Figure 3**.

Molecule	HOMO	LUMO
KTZ		
CTZ		
TBZ		
		

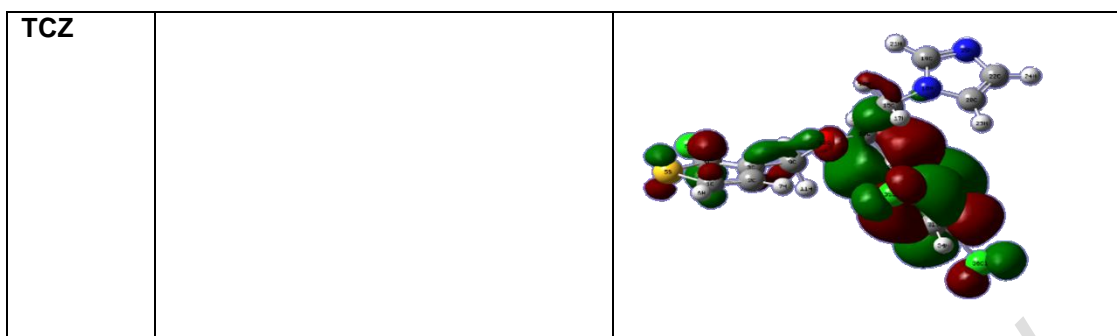


**Figure 3 HOMO and LUMO orbitals of KTZ, CTZ, TBZ and TCZ using DFT at B3LYP/6-31G (d).**

By analyzing the HOMO–LUMO energy gap values for these molecular compounds in table 1, it can be noted that TBZ has the lowest energy gap value. Therefore this compound can be predicted to be best corrosion inhibitor compared to other molecules studied. Indeed when the value of  $\Delta E$  is low, the electronic transfer between HOMO and LUMO orbitals is easier [32,33]. This good inhibition performance that TBZ could possess is due to the presence of heteroatoms (N, S) and  $\pi$  bonds able to ensure a good interaction between the metal and the molecules.

Referring to the table, all the molecules studied have a low electronegativity value compared to that of copper ( $\chi_{Cu}=4.98$  eV). In this case the movement of electrons will be from each molecule to the metal. It appears therefore that the ability of these molecules to protect copper against corrosion will be by receiving their electrons. In fact, the electron flow will happen from the system with the low electronegativity towards that of a higher value until the chemical potentials are the same [23].

We can observe from Table 1 that the hardness ( $\eta$ ) values of the studied compounds are in the following order:  $\eta(TBZ) < \eta(KTZ) < \eta(TCZ) < \eta(CTZ)$ . This order is the reverse of that obtained for global softness. Thus, the inhibitor with the least value of global hardness (hence the highest value of global softness) could have the best inhibitory performance in controlling copper corrosion in acidic media. In this case TBZ could protect the copper better against corrosion than the other compounds studied

$\Delta N$  values of the studied compounds are lower than 3.6. It follows in this case that these compounds give electrons to copper in order to strengthen its surface [34]. In fact during the corrosion of copper, it loses electrons. In order to protect it, each compound will give electrons to compensate for the lost electrons.

The studied molecules can be good inhibitors for copper corrosion because on the one hand the unoccupied d orbitals of  $Cu^{2+}([Ar]3d^9)$  can accept electrons from the inhibitors to form a coordination bond. On the other hand, the inhibitor molecules can accept electrons from the  $Cu^{2+}$  ion with a coordination bond. These donation and back donation processes strengthen the adsorption of the inhibitors molecules onto copper surface

The total energy values are all negative, this implies that the transfer of electrons metal-molecule is possible [35,36].

### 3.3 Local reactivity parameters Analysis

In order to locate the sites capable of donating or accepting electrons the Mulliken charges and Fukui indices of each molecule were calculated [37-40]. In addition, the dual descriptors were also determined in order to unambiguously locate the active sites of the inhibitor molecules. The results are grouped in tables 2,3,4 and 5. The analysis of these results will allow to understand the interactions of each inhibitor with the metal.

**Table 2. Mulliken atomic charges, Fukui indices and dual descriptor of KTZ DFT using DFT at B3LYP/6-31G (d)**

Atoms	$q_k(N + 1)$	$q_k(N)$	$q_k(N - 1)$	$f_k^+$	$f_k^-$	$\Delta f_k(r)$
1 C	-0.008043	0.575909	0.012710	-0.583952	0.563199	<b>-1.147151</b>
2 O	0.017543	-0.506838	0.004915	0.524381	-0.511753	1.036134
3 C	0.000552	-0.549299	-0.001201	0.549851	<b>-0.548098</b>	1.097949
4 H	-0.000195	0.168155	0.000925	-0.168350	0.167230	-0.335580
5 H	-0.000071	0.189323	0.000032	-0.189394	0.189291	-0.378685
6 H	-0.000277	0.167769	0.001297	-0.168046	0.166472	-0.334518
7 C	0.006127	-0.144312	-0.000291	0.150439	-0.144021	0.294460
8 C	-0.000231	-0.141538	-0.000040	0.141307	-0.141498	0.282805
9 C	-0.015238	-0.136170	0.000744	0.120932	-0.136914	0.257846
10 H	0.004257	0.148743	0.001154	-0.144486	0.147589	-0.292075
11 H	-0.000050	0.194712	-0.000051	-0.194762	0.194763	-0.389525
12 C	-0.009774	-0.132965	0.001238	0.123191	-0.134203	0.257394
13 H	0.005975	0.152318	0.000546	-0.146343	0.151772	-0.298115
14 H	-0.000474	0.159486	0.000001	-0.159960	0.159485	-0.319445
15 H	0.001118	0.156714	0.002786	-0.155596	0.153928	-0.309524
16 H	0.027730	0.134635	-0.000200	-0.106905	0.134835	-0.241740
17 H	0.000584	0.156685	0.002371	-0.156101	0.154314	-0.310415
18 H	0.031058	0.134527	-0.000409	-0.103469	0.134936	-0.238405
19 N	0.030384	-0.423317	-0.000891	0.453701	-0.422426	0.876127
<b>20 N</b>	0.310112	-0.503597	-0.000757	<b>0.813709</b>	-0.502840	<b>1.316549</b>
21 C	0.043237	0.328785	-0.024233	-0.285548	0.353018	-0.638566



22	C	0.079125	-0.178086	0.094625	0.257211	-0.272711	0.529922
23	C	0.072460	-0.195317	0.059622	0.267777	-0.254939	0.522716
24	C	-0.037948	-0.173642	0.071123	0.135694	-0.244765	0.380459
25	H	-0.003578	0.134319	-0.005516	-0.137897	0.139835	-0.277732
26	C	-0.017413	-0.177690	0.092555	0.160277	-0.270245	0.430522
27	H	-0.003641	0.135763	-0.003699	-0.139404	0.139462	-0.278866
28	C	0.144381	0.352328	-0.026517	-0.207947	0.378845	-0.586792
29	H	0.001074	0.145943	-0.001707	-0.144869	0.147650	-0.292519
30	H	0.000622	0.133315	-0.005546	-0.132693	0.138861	-0.271554
31	O	0.028580	-0.543523	0.000202	0.572103	-0.543725	1.115828
32	C	0.003871	-0.025738	0.000775	0.029609	-0.026513	0.056122
33	H	-0.000161	0.151449	0.001444	-0.151610	0.150005	-0.301615
34	H	0.002836	0.131351	-0.000184	-0.128515	0.131535	-0.260050
35	C	0.000430	0.087967	-0.000718	-0.087537	0.088685	-0.176222
36	C	0.000090	-0.062528	0.000519	0.062618	-0.063047	0.125665
37	H	-0.000042	0.163990	0.000763	-0.164032	0.163227	-0.327259
38	C	0.000266	0.468778	-0.000061	-0.468512	0.468839	-0.937351
39	H	0.000112	0.167708	0.000242	-0.167596	0.167466	-0.335062
40	H	0.000550	0.150445	0.000446	-0.149895	0.149999	-0.299894
41	O	0.002972	-0.510863	0.003940	0.513835	-0.514803	1.028638
42	O	0.000037	-0.513438	0.003260	0.513475	-0.516698	1.030173
43	C	-0.000042	-0.158424	0.014025	0.158382	-0.172449	0.330831
44	H	-0.000086	0.178099	-0.000676	-0.178185	0.178775	-0.356960
45	H	0.000174	0.168733	0.010427	-0.168559	0.158306	-0.326865
46	N	-0.013430	-0.373661	-0.001262	0.360231	-0.372399	0.732630
47	C	0.114900	0.198498	0.000291	-0.083598	0.198207	-0.281805

48	C	0.125796	0.004832	0.000153	0.120964	0.004679	0.116285
49	H	-0.005636	0.154261	-0.000093	-0.159897	0.154354	-0.314251
50	C	0.091436	-0.037201	0.000068	0.128637	-0.037269	0.165906
51	H	-0.005351	0.156774	0.000035	-0.162125	0.156739	-0.318864
52	H	-0.004638	0.135526	0.000014	-0.140164	0.135512	-0.275676
53	N	-0.024581	-0.435374	0.000582	0.410793	-0.435956	0.846749
54	C	0.000418	0.089263	0.283483	-0.088845	-0.194220	0.105375
55	C	-0.000186	-0.170870	0.072552	0.170684	-0.243422	0.414106
56	C	0.001486	-0.142347	0.011112	0.143833	-0.153459	0.297292
57	C	0.000508	-0.077627	-0.020696	0.078135	-0.056931	0.135066
58	H	0.000027	0.185566	-0.004823	-0.185539	0.190389	-0.375928
59	C	0.000008	-0.074801	0.043612	0.074809	-0.118413	0.193222
60	H	-0.000187	0.182826	-0.001753	-0.183013	0.184579	-0.367592
61	C	0.000070	-0.122688	0.326728	0.122758	-0.449416	0.572174
62	H	-0.000002	0.178012	-0.018920	-0.178014	0.196932	-0.374946
63	Cl	0.000155	-0.001910	-0.000460	0.002065	-0.001450	0.003515
64	Cl	0.000213	-0.009747	-0.000614	0.009960	-0.009133	0.019093

**Table 3. Mulliken atomic charges, Fukui indices and dual descriptor of CTZ DFT using DFT at B3LYP/6-31G (d)**

Atoms	$q_k(N+1)$	$q_k(N)$	$q_k(N-1)$	$f_k^+$	$f_k^-$	$\Delta f_k(r)$
1 C	0.046440	-0.158170	0.068410	0.204610	-0.226580	0.431190
2 C	-0.005050	-0.126960	-0.022550	0.121910	-0.104410	0.226320
3 C	0.013480	0.097180	0.075040	-0.083700	0.022140	-0.105840
4 C	0.037600	-0.298270	0.104440	0.335870	-0.402710	0.738580
5 C	-0.000652	-0.113810	-0.036950	0.113158	-0.076860	0.190018
6 C	0.006880	-0.128870	0.092370	0.135750	-0.221240	0.356990

---

7	H	-0.001930	0.132150	-0.004210	-0.134080	0.136360	-0.270440
8	H	-0.000268	0.147160	0.001030	-0.147428	0.146130	-0.293558
9	H	-0.001570	0.181010	-0.005580	-0.182580	0.186590	-0.369170
10	H	-0.000161	0.132660	0.001600	-0.132821	0.131060	-0.263881
11	H	-0.000433	0.132510	-0.005650	-0.132943	0.138160	-0.271103
12	C	-0.013480	0.000974	0.021260	-0.014454	-0.020286	0.005832
13	C	0.087180	0.105740	0.073460	-0.018560	0.032280	-0.050840
14	C	0.063790	-0.206790	0.119920	0.270580	-0.326710	0.597290
15	C	-0.028510	-0.134390	-0.027780	0.105880	-0.106610	0.212490
16	C	-0.026250	-0.135870	-0.039430	0.109620	-0.096440	0.206060
17	H	-0.002830	0.163300	-0.006960	-0.166130	0.170260	-0.336390
18	C	0.057860	-0.151460	0.081050	0.209320	-0.232510	0.441830
19	H	0.000652	0.155780	0.000405	-0.155128	0.155375	-0.310503
20	C	0.060760	-0.128470	0.097290	0.189230	-0.225760	0.414990
21	H	0.000713	0.138450	0.001300	-0.137737	0.137150	-0.274887
22	H	-0.002480	0.138570	-0.005080	-0.141050	0.143650	-0.284700
23	H	-0.002680	0.135370	-0.005970	-0.138050	0.141340	-0.279390
24	C	0.064510	0.115430	0.089320	-0.050920	0.026110	-0.077030
25	C	0.011720	-0.207190	0.164270	0.218910	-0.371460	0.590370
26	C	-0.000983	-0.097570	-0.045950	0.096587	-0.051620	0.148207
27	C	-0.008010	-0.126560	-0.033160	0.118550	-0.093400	0.211950
28	C	0.001500	-0.183930	0.144170	0.185430	-0.328100	0.513530
29	H	-0.001550	0.199950	0.001340	-0.201500	0.198610	-0.400110
30	C	0.041020	-0.122150	0.082090	0.163170	-0.204240	0.367410
31	H	0.000200	0.154280	0.000956	-0.154080	0.153324	-0.307404
32	H	-0.000142	0.146160	-0.008480	-0.146302	0.154640	-0.300942

---

33	H	-0.001700	0.143920	-0.005480	-0.145620	0.149400	-0.295020
34	Cl	0.011890	0.089640	0.004560	-0.077750	0.085080	-0.162830
35	N	0.008430	-0.420140	0.006860	<b>0.428570</b>	-0.427000	<b>0.855570</b>
36	C	0.229250	0.127910	0.006150	0.101340	0.121760	-0.020420
37	C	0.208730	0.020520	0.002090	0.188210	0.018430	0.169780
38	H	0.230390	-0.025840	0.000542	0.256230	-0.026382	0.282612
39	C	-0.010740	0.199150	-0.000502	-0.209890	<b>0.199652</b>	<b>-0.409542</b>
40	H	-0.008880	0.175420	0.001480	-0.184300	0.173940	-0.358240
41	H	-0.011170	0.150640	0.000544	-0.161810	0.150096	-0.311906
42	N	-0.053520	-0.417440	0.011800	0.363920	-0.429240	0.793160

**Table 4.**Mulliken atomic charges,Fukui indices and dual descriptor of TBZ DFT using DFT at B3LYP/6-31G (d)

Atoms	$q_k(N + 1)$	$q_k(N)$	$q_k(N - 1)$	$f_k^+$	$f_k^-$	$\Delta f_k(r)$
1 C	0.296933	-0.148547	0.084021	0.445480	-0.232568	0.678048
2 C	-0.092226	-0.173826	0.063758	0.081600	-0.237584	0.319184
3 C	0.167686	0.357305	-0.018143	-0.189619	<b>0.375448</b>	-0.565067
4 C	0.135371	0.237262	-0.015418	-0.101891	0.252680	-0.354571
5 C	0.071703	-0.182972	0.129682	0.254675	-0.312654	0.567329
6 C	-0.020661	-0.142239	-0.037296	0.121578	-0.104943	0.226521
7 H	-0.013039	0.127719	-0.005038	-0.140758	0.132757	-0.273515
8 H	0.002954	0.126107	-0.003950	-0.123153	0.130057	-0.253210
9 H	-0.003990	0.143244	-0.006694	-0.147234	0.149938	-0.297172
10 H	-0.000103	0.127025	0.001170	-0.127128	0.125855	-0.252983
11 C	0.140353	0.487276	0.137379	-0.346923	0.349897	<b>-0.696820</b>
12 N	-0.039596	-0.765538	0.024209	<b>0.725942</b>	-0.789747	<b>1.515689</b>
13 H	0.000752	0.327890	0.000615	-0.327138	0.327275	-0.654413

14 N	0.086376	-0.532410	0.056077	0.618786	-0.588487	1.207273
15 C	0.030498	0.265186	0.019340	-0.234688	0.245846	-0.480534
16 C	0.163800	-0.400414	0.433023	0.564214	-0.833437	1.397651
17 C	0.040562	-0.117466	0.101133	0.158028	-0.218599	0.376627
18 N	-0.012013	-0.361397	-0.036472	0.349384	-0.324925	0.674309
19 H	-0.007933	0.175801	-0.024772	-0.183734	0.200573	-0.384307
20 H	-0.002257	0.191367	-0.006685	-0.193624	0.198052	-0.391676
21 S	0.054829	0.258626	0.104061	-0.203797	0.154565	-0.358362

**Table 5. Mulliken atomic charges, Fukui indices and dual descriptor of TCZ DFT using DFT at B3LYP/6-31G (d)**

Atoms	$q_k(N+1)$	$q_k(N)$	$q_k(N-1)$	$f_k^+$	$f_k^-$	$\Delta f_k(r)$
1 C	0.183028	-0.36171	0.104877	<b>0.544738</b>	-0.466587	1.011325
2 C	-0.007783	-0.09464	-0.010105	0.086857	-0.084535	0.171392
3 C	0.052624	0.1613	0.026748	-0.108676	0.134552	-0.243228
4 C	0.170657	-0.35665	0.163793	0.527307	-0.520443	<b>1.04775</b>
5 S	-0.030862	0.30463	0.045116	-0.335492	<b>0.259514</b>	<b>-0.595006</b>
6 H	-0.008462	0.18412	-0.006456	-0.192582	0.190576	-0.383158
7 H	-0.000251	0.16843	0.000522	-0.168681	0.167908	-0.336589
8 Cl	0.068457	0.02562	0.001388	0.042837	0.024232	0.018605
9 C	-0.003396	-0.08773	0.007305	0.084334	-0.095035	0.179369
10 H	0.001878	0.14918	-0.0004	-0.147302	0.14958	-0.296882
11 H	0.005323	0.15619	0.002794	-0.150867	0.153396	-0.304263
12 O	0.006846	-0.48606	0.008154	0.492906	-0.494214	0.98712
13 C	-0.000427	0.08186	0.018161	-0.082287	0.063699	-0.145986
14 H	-0.000135	0.13564	-0.000595	-0.135775	0.136235	-0.27201
15 C	0.00522	-0.19138	0.00977	0.1966	-0.20115	0.39775

16	H	0.000942	0.18267	0.004681	-0.181728	0.177989	-0.359717
17	H	-0.000027	0.19096	0.000072	-0.190987	0.190888	-0.381875
18	N	-0.01496	-0.37081	-0.000212	0.35585	-0.370598	0.726448
19	C	0.192777	0.18863	0.000446	0.004147	0.188184	-0.184037
20	C	0.17348	0.00902	0.000568	0.16446	0.008452	0.156008
21	H	-0.009397	0.1511	0.000105	-0.160497	0.150995	-0.311492
22	C	0.176096	-0.04164	0.000428	0.217736	-0.042068	0.259804
23	H	-0.007427	0.15652	-0.000181	-0.163947	0.156701	-0.320648
24	H	-0.008563	0.13547	-0.000031	-0.144033	0.135501	-0.279534
25	N	-0.051831	-0.43455	0.000043	0.382719	-0.434593	0.817312
26	C	0.043082	0.15571	0.220647	-0.112628	-0.064937	-0.047691
27	C	-0.003144	-0.1777	-0.01918	0.174556	-0.15852	0.333076
28	C	0.008378	-0.13388	0.150551	0.142258	-0.284431	0.426689
29	C	0.010219	-0.12074	0.089913	0.130959	-0.210653	0.341612
30	H	-0.000139	0.15942	-0.000357	-0.159559	0.159777	-0.319336
31	C	-0.003627	-0.12687	-0.076773	0.123243	-0.050097	0.17334
32	C	0.025963	-0.06292	0.258173	0.088883	-0.321093	0.409976
33	H	-0.000496	0.16861	-0.006203	-0.169106	0.174813	-0.343919
34	H	0.000035	0.18155	0.002656	-0.181515	0.178894	-0.360409
35	Cl	0.006352	-3.10E-05	0.001145	0.006383	-0.001176	0.007559
36	Cl	0.01957	6.69E-04	0.002438	0.018901	-0.001769	0.02067

The probable sites for nucleophilic attacks are the sites for which the values of the Fukui index  $f_k^+$  and the dual descriptor are the largest. As for the electrophilic attack sites, they are

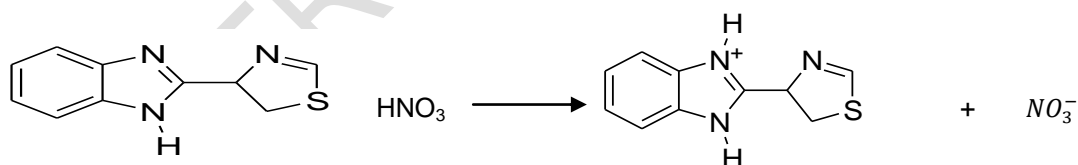
identified by the largest value of the Fukui index  $f_k^-$  and by the smallest value of the dual descriptor  $\Delta f_k(r)$ . In case of ambiguity the atom with the largest value and the smallest value of  $\Delta f_k(r)$  for the same compound are respectively the probable sites for nucleophilic and electrophilic attacks. Thus in view of the above and after analysis tables 2, 3, 4 and 5, the different sites of reactivity of the studied molecules are recorded in table 6.

**Table.6 Recap of the different reactivity atoms**

Molecules	probable sites for nucleophilic	probable sites for electrophilic
KTZ	N(20)	C(1)
CTZ	N(35)	C(39)
TBZ	N(12)	C(11)
TCZ	C(4)	S(5)

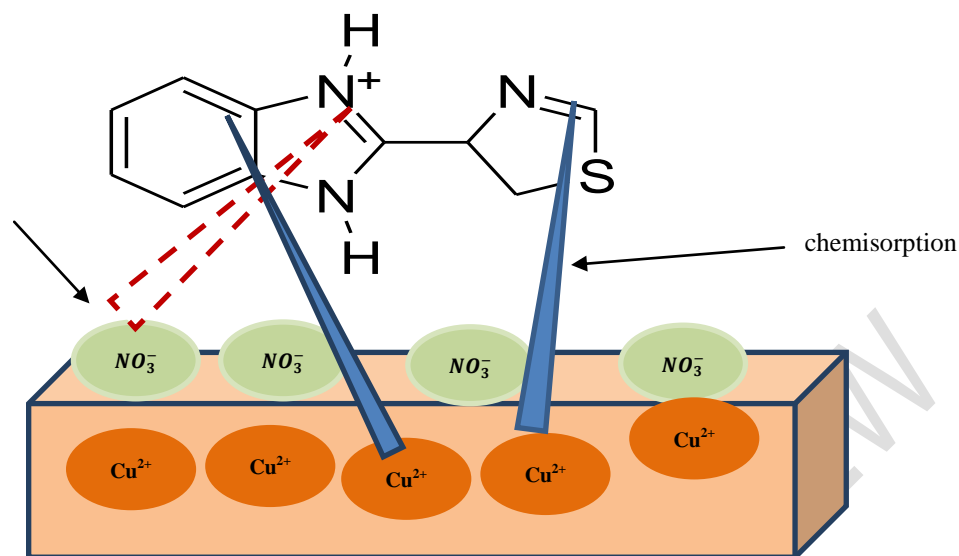
It appears that the reactivity of the studied inhibitors strongly depends on N,S heteroatoms and C carbon atom. However the probable sites for nucleophilic attacks are dominated by nitrogen atoms (N). In addition these sites associated with the LUMO orbital could receive electrons that would come from the metal. Regarding the probable sites for electrophilic attacks, they are dominated by carbon atoms (C) with the presence of a sulfur atom (S). These sites are likely to donate electrons to the metal. The donor-acceptor properties that these molecules possess give them a good ability to protect copper against corrosion in nitric acid solution.

The inhibitor molecules are protonated in nitric acid medium. Thiabendazole is protonated according to the chemical in following equation:



The inhibitor molecule protonated formed in the solution will allow the compound to adsorb on the copper surface negatively charged by  $\text{NO}_3^-$  ions. Thanks to the charge carried by the proton, the latter, interacting with the negative charge of the nitrate ions, gives rise to electrostatic interactions that promote physisorption. The free electron pairs of the heteroatoms belong to each compound studied, as well as the  $\pi$  electrons of the aromatic rings which help the molecule to adsorb on copper surface. This adsorption is facilitated by the presence of the unfilled d-orbitals gives importance to the donor-acceptor interactions between the molecule and the metal surface favoring the chemisorption.

Figure 4 explains the mechanism of adsorption.



## Conclusion

Quantum chemical studies justified by DFT calculations revealed that the inhibitory power of KTZ, CTZ, TBZ and TCZ is promoted by their electron donor-acceptor ability. These inhibition properties could strengthen the copper surface by reducing its degradation. The energy gap, softness and hardness indicate that TBZ could have the best inhibitory performance in copper corrosion in the studied solution. The total energy values of the studied compounds predict that the electronic exchanges between them and copper are favorable. In addition, the values of Fukui indices and dual descriptor led to accurate predictions of the positions for electrophilic and nucleophilic attack. These positions also estimated the importance of nitrogen, carbon and sulfur atoms in the local reactivity.

## References

1. Zhang T., Yongming T., Ziyi C., Wenheng J., Zhenglei W. and Yizhong C. Performance and theoretical study on corrosion inhibition of 2-(4-pyridyl) benzimidazole for mild steel in hydrochloric acid. *Corrosion Science*. 2012, 61: 1-9.
2. Niamien PM, Essy F K, Trokourey A, Yapi A, Aka H.K. and Diabate D. Correlation between the molecular structure and the inhibiting effect of some benzimidazole derivatives. *Materials Chemistry and Physics*. 2012, 136(1):59-65.
3. Tigori M.A., Kouyaté A., Kouakou V, Niamien P.M. and Trokourey A., Computational approach for predicting the adsorption properties and inhibition of some antiretroviral drugs on copper corrosion in HNO<sub>3</sub>, *European Journal of Chemistry*. 2020; 11(3): 235-244.
4. Tigori, M.A., Kouyaté, A., Kouakou, V., Niamien, P.M. and Trokourey, A., Inhibition Performance of Some Sulfonyleurea on Copper Corrosion in Nitric Acid Solution Evaluated Theoretically by DFT Calculations, *Open Journal of Physical Chemistry*, 2020, 10(3):139-157.
5. Yesim S. Kara, Seda G. Sagdinc and Asli Esme. Theoretical study on the relationship between the molecular structure and corrosion inhibition efficiency of



long alkyl side chain acetamide and isoxazolidine derivatives. *Protection of Metals and Physical Chemistry of Surfaces*, 2012, 48(6):710-721.

6. Yadav M., Debasis B., Sumit K. and Rajesh R. S. Experimental and Quantum Chemical Studies on the Corrosion Inhibition Performance of Benzimidazole Derivatives for Mild Steel in HCl. *Industrial & Engineering Chemistry Research*. 2013, 52(19):6318-6328.
7. Hassane Lgaz, Ill-Min Chung, Mustafa R. Albayati, Abdelkarim Chaouiki, Rachid Salghi and Shaaban K. Mohamed. (2020) Improved corrosion resistance of mild steel in acidic solution by hydrazone derivatives: An experimental and computational study. *Arabian Journal of Chemistry*. 2020, 13(1):2934-2954.
8. Khattabi M., Benhiba F., Tabti S., Djedouani A., El Assyry A., Touzani R., Warad I., Oudda H. and Zarrouk A. Performance and computational studies of two soluble pyran derivatives as corrosion inhibitors for mild steel in HCl. *Journal of Molecular Structure*. 2019; 1196: 231-244.
9. Eddy, N.O., Momoh-Yahaya, H. and Oguzie, E.E. Theoretical and Experimental Studies on the Corrosion Inhibition Potentials of Some Purines for Aluminium in 0.1 M HCl. *Journal of Advanced Research*. 2015, 6:203-217.
10. Tecuapa-Flores E.D., Turcio-Ortega D., Guadalupe Hernandez J., Huerta-Aguilar C. A. and Thangarasu P. The role of keto group in cyclic ligand 1,4,8,11-tetraazacyclotetradecane-5,7-dione as strong corrosion inhibitor for carbon steel surface: Experimental and theoretical studies. *Journal of Molecular Structure*. 2019; 1189:131-145.
11. Qiang Y, Zhang S, Yan S, Zou X, Chen S., Three indazole derivatives as corrosion inhibitors of copper in a neutral chloride solution, *Corrosion Science*. 2017; 126: 295–304.
12. Hosseini S. M. A. and Azimi A., "The inhibition of mild steel corrosion in acidic medium by 1-methyl-3-pyridin-2-ylthiourea," *Corrosion Science*, 2009; 51(4): 728–732.
13. Okafor P. C. and Zheng Y, Synergistic inhibition behaviour of methylbenzyl quaternary imidazoline derivative and iodide ions on mild steel in H<sub>2</sub>SO<sub>4</sub> solutions, *Corrosion Science*. 2009, 51(4):850–859, 2009.
14. Singh A.K. and Quraishi M.A. Effect of Cefazolin on the Corrosion of Mild Steel in HCl Solution. *Corrosion Science*. 2009; 52, 152-160. <https://doi.org/10.1016/j.corsci.2009.08.050>
15. Alagarsamy V.; Solomon V.R.; Dhanabal K. Synthesis and pharmacological evaluation of some 3-phenyl-2-substituted-3H-quinazolin-4-one as analgesic, anti-inflammatory agents. *Bioorganic & Medicinal Chemistry*. 2007, 15, 235–241.
16. Frisch M. J.; Trucks, G. W.; Schlegel, H. B. , Scuseria, G. E.; Robb, M. A.; Cheeseman, J. R.; Scalmani, G.; Barone, V.; Mennucci, B.; Petersson, G. A.; Nakatsuji, H.; Caricato, M.; Li, X.; Hratchian, H. P.; Izmaylov, A. F.; Bloino, J.; Zheng, G.; Sonnenberg, J. L.; Hada, M. , Ehara, M.; Toyota, K.; Fukuda, R.; Hasegawa, J.; Ishida, M.; Nakajima, T.; Honda, Y.; Kitao, O.; Nakai, H.; Vreven, T.;

Montgomery, Jr.; Peralta, J. E.; Ogliaro, F.; Bearpark, M.; Heyd, J. J.; Brothers, E.; Kudin, K. N.; Staroverov, V. N.; Kobayashi, R.; Normand, J.; Raghavachari, K.; Rendell, A.; Burant, J. C.; Iyengar, S. S.; Tomasi, J.; Cossi, M.; Rega, N.; Millam, J. M.; Klene, M.; Knox, J. E.; Cross, J. B.; Bakken, V.; Adamo, C.; Jaramillo, J.; Gomperts, R.; Stratmann, R. E.; Yazyev, O.; Austin, A. J.; Cammi, R.; Pomelli, C.; Ochterski, J. W.; Martin, R. L.; Morokuma, K.; Zakrzewski, V. G.; Voth, P. Salvador, G. A.; Dannenberg, S. Dapprich, J. J.; Daniels, A. D.; Farkas, Ö.; Foresman, J. B.; Ortiz, J. V.; Cioslowski J.; Fox, A. D. J. Gaussian 09. Gaussian, Inc., Wallingford, CT, 2009.

17. Yang W., Parr R. G., "Hardness, softness, and the fukui function in the electronic theory of metals and catalysis" proceeding of the National Academy of Sciences. 1985, 82(20):6723-6726.
18. N. Lopez and F. Illas, "Ab initio modeling of the metal-support interface: the interaction of Ni, Pd, and Pt on MgO(100)," Journal of Physical Chemistry B, 1998, 102(8):1430–1436.
19. Koopmans, T. (1934) About the Assignment of Wave Functions and Eigenvalues to the Individual Electrons of Atoms. Über die Zuordnung von Wellenfunktionen und Eigenwerten zu den Einzelnen Elektronen Eines Atoms. Physica, 1934, 1:104-113.
20. Parr, R.G. and Yang, W. Absolute Hardness: Comparison Parameter to Absolute Electronegativity Journal of the American Chemical Society. 1983, 105: 7512-7516.
21. Yang W. and Parr R.G. Absolute Electronegativity and Hardness Correlated with Molecular Orbital Theory. Proceeding of the National Academy of Sciences. 1986; 83, 8440-8441.
22. Parr R.G., Szentpaly L. and Liu S. Electrophilicity Index. Journal of the American Chemical Society. 1999, 121:1922-1924.
23. Pearson R.G. Absolute Electronegativity and Hardness: Application to Inorganic Chemistry. Inorganic Chemistry. 1988, 27, 734-740.
24. Michaelson H.B. The Work Function of the Elements and Its Periodicity. Journal of Applied Physics. 1977, 48:4729-4733.
25. Dewar M.J.S., Zoebisch E.G., Healy E.F. and Stewart J.P. Development and Use of Quantum Mechanical Molecular Models, 76, AM1: A New General Purpose Quantum Mechanical Molecular Model. Journal of the American Chemical Society. 1985, 107:3902-3909.
26. Martínez-Araya J.I., Why the dual descriptor is a more accurate local reactivity descriptor than Fukui functions? journal of Mathematical Chemistry , 2015, 53: 451-465.
27. Morell, C.; Grand, A.; Toro Labbe, A. .New Dual Descriptor for Chemical Reactivity. Journal of Physical Chemistry. A, 2004, 109(1): 205-212.
28. Musa A. Y., Kadhum A. A. H., Mohamad A. B., Rahoma A. A. B., and Mesmari H., Electrochemical and quantum chemical calculations on 4,4-dimethyloxazolidine-2-

thione as inhibitor for mild steel corrosion in hydrochloric acid. *Journal of Molecular Structure*. 2010, 969(1–3): 233–237.

29. Abdelqader E. G., Abderrahim T., Karima C. Naoual M., Mohamed El A., Rachid T., Belkheir H. and Hassane L. The Synergistic Effect of Chloride Ion and 1,5-Diaminonaphthalene on the Corrosion Inhibition of Mild Steel in 0.5 M Sulfuric Acid: Experimental and Theoretical Insights. *Surfaces and Interfaces*. 2018, 13:168-177.
30. Ahamad I., Prasad R. and Quraishi M.A., Adsorption and inhibitive properties of some new Mannich bases of Isatin derivatives on corrosion of mild steel in acidic media. *Corrosion Science*. 2010, 52(4):1472-1481.
31. Loutfy H. Madkour S. Kaya, Lei G. and Cemal K.. Quantum chemical calculations, molecular dynamic (MD) simulations and experimental studies of using some azo dyes as corrosion inhibitors for iron. Part 2: Bis-azo dye derivatives. *Journal of Molecular Structure*. 2018, 1163:397-417.
32. Singh A, Ansari K.R.; A Kumar A; Liu W.; Songsong C.; Liu Y. Electrochemical, surface and quantum chemical studies of novel imidazole derivatives as corrosion inhibitors for J55 steel in sweet corrosive environment. *Journal of Alloys and Compounds*. 2017, 72:121-133.
33. Reza Teimuri-Mofrad, Iraj Ahadzadeh, Mahdi Gholamhosseini-Nazari, Somayeh Esmati and Aziz Shahriza. Synthesis of Betti base derivatives catalyzed by nano-CuO-ionic liquid and experimental and quantum chemical studies on corrosion inhibition performance of them. *Research on Chemical Intermediates*. 2018; 44(4):2913-2927.
34. Lukovits I., Kalman E. and Zucchi F. Corrosion Inhibitors-Correlation between Electronic Structure and Efficiency. *Corrosion*. 2001; 57: 3-8.
35. Nwankwo H.U., Olasunkanmi L.O. and Ebenso E.E Experimental, Quantum Chemical and Molecular Dynamic Simulations Studies on the Corrosion Inhibition of Mild Steel by Some Carbazole Derivatives. *Scientific Report*. 2017, 7:2436-2446.
36. Mohamed E. F., Fouad B. , Hafida A. , Younes K. , Abdellah G. , Brahim L. , Ismail W., Chandrabhan V. , El-Sayed M. S. , Ebenso E. E., Zarrouk A . Experimental and computational investigations on the anti-corrosive and adsorption behavior of 7-N,N'-dialkylaminomethyl-8-Hydroxyquinolines on C40E steel surface in acidic medium, *Journal of Colloid and Interface Science*. 2020; 576: 330–344.
37. Hong J., Li X., Cao N., Wang F., Liu Y. and Li Y. Schiff-base derivatives as corrosion inhibitors for carbon steel materials in acid media: quantum chemical calculations. *Corrosion Engineering, Science and Technology*. 2018, 53:1, 36-43.
38. Kouakou V., Niamien P. M., Yapo A. J. and Trokourey A, Copper Corrosion Inhibition in 1M Nitric Acid: Adsorption and Inhibitive Action of Théophylline. *Chem Science Review and Letter*. 2016; 5(20):131-146.
39. Lei Guo , Shanhong Zhu , Shengtao Zhang , Qiao He , Weihua Li , theoretical studies of three triazole derivatives as corrosion inhibitors for mild steel in acidic medium, *Corrosion Science*. 2014, 87:366–375.

40. Lei Guo L., Kaya S., Obot I.B., Zheng X. and Qiang Y. Toward understanding the anticorrosive mechanism of some thiourea derivatives for carbon steel corrosion: A combined DFT and molecular dynamics investigation. *Journal of Colloid and Interface Science*. 2017, 506, 478-485.

UNDER PEER REVIEW